Available online at www.sciencedirect.com

ScienceDirect

Scripta Materialia 106 (2015) 52–56

Scripta MATERIALIA

www.elsevier.com/locate/scriptamat

Comments and Reply

Micromechanisms associated with the dynamic compressive failure of hot-pressed boron carbide

L. Farbaniec,[a] J.D. Hogan[a] and K.T. Ramesh[a,b,*]

[a]*Hopkins Extreme Materials Institute, The Johns Hopkins University, Baltimore, MD 21218, USA*
[b]*Department of Mechanical Engineering, The Johns Hopkins University, Baltimore, MD 21218, USA*

Received 19 February 2015; revised 23 April 2015; accepted 2 May 2015
Available online 27 May 2015

Brittle failure in boron carbide has been studied in dynamic uniaxial compression using a Kolsky bar technique. A detailed study of fragments was performed using SEM-EDS, to identify the mechanisms responsible for failure. Microstructural characterization and fracture surface observations revealed that carbon inclusions oriented at certain angles with respect to the direction of loading might act as possible crack initiation sites. Cracks developed from these inhomogeneities had a tensile character, and were linked to the wing crack mechanism.

Keywords: Boron carbide; Brittle failure; Wing cracks; Kolsky bar technique

Boron carbide is an attractive advanced ceramic because of its low density, excellent hardness and wear resistance [1,2]. As with many other ceramics, the processing of pure boron carbide to high densities requires different additives for better densification [1,3–5]. The consolidated material can also contain non-oxide impurities like free carbon, which acts also as a sintering aid [5–7]. All of these can form secondary phases or precipitates at the grain boundaries or within the grains. Cracks can initiate from these inhomogeneities, and their subsequent propagation is strongly coupled to the highly inhomogeneous and evolving fields ahead of the crack tips, and perhaps by other cracks in the vicinity. These failure mechanisms have been extensively studied for many years in failure of brittle solids [8–12]. However, fundamental issues related to the dynamic nucleation and propagation of cracks are poorly understood for advanced ceramics.

In previous work [13], we investigated the rate-dependent compressive failure and fragmentation of a hot-pressed boron carbide using quantitative fragment analysis. In the current study, we investigate the impact of the pre-existing microstructural inhomogeneities on microcracking and failure mechanisms in hot-pressed boron carbide through a detailed microstructural characterization. The experiments were conducted using commercial hot-pressed boron carbide (CoorsTek, Inc.) with a density of 2.51 g/cm^3, and equiaxed grains with an average size of ~15 μm, as provided by the manufacturer. Prior to testing, the microstructure was characterized to determine the mesoscale inhomogeneities of interest by using a TESCAN MIRA3 field emission Scanning Electron Microscope (SEM) coupled with Energy Dispersive Spectrometry (EDS). A chemical composition analysis was carried out with the resolution of 0.5 μm. Identified microstructural inhomogeneities such as carbon, aluminum nitride and boron nitride inclusions were afterward quantified and measured by taking a series of optical microscopy images treated with image processing tools developed in Matlab software (MathWorks, Inc.) [13].

The Kolsky bar experimental setup used in this study, and the testing procedure for ceramic materials is presented in [14]. The compression specimens (with dimensions of 3.5 mm × 4 mm × 5.3 mm) were cut from a plate 8 mm thick with the loading axis parallel to the hot-pressing direction. For the purposes of subsequent discussion, the coordinate system (X_1, X_2 and X_3) is associated with the specimen in the following manner: X_3 is the hot-pressing (and compressive loading) direction; X_1 and X_2 are principal directions lying in the hot-pressed surface. The dynamic compression tests were carried out at a strain-rate of ~10^3 s^{-1}. To understand the failure mechanisms, the collected fragments of the specimens were investigated by SEM-EDS and optical microscopy with image processing.

Figure 1(a and b) shows optical micrographs of the microstructure in two representative planes, where (1a) shows a plane normal to the hot-pressing direction and (1b) shows a plane through the thickness of the material

* Corresponding author at: Hopkins Extreme Materials Institute, The Johns Hopkins University, Baltimore, MD 21218, USA; e-mail: ramesh@jhu.edu

http://dx.doi.org/10.1016/j.scriptamat.2015.05.004
1359-6462/

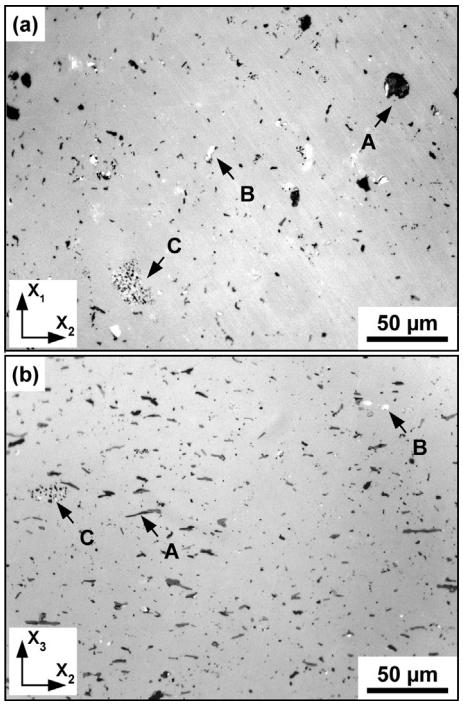

Figure 1. (a and b) Optical microscope image of boron carbide microstructure in two representative planes. Characteristic inhomogeneities, such as free carbon (A), other non-metallic inclusions such as aluminum nitride, boron nitride (B) and pores (C) are indicated.

and containing the hot-pressing direction (vertical in this case). Three different characteristic inhomogeneities can be distinguished from these images: free carbon (labeled 'A'), other non-metallic inclusions, identified later as aluminum nitride and boron nitride (labeled 'B'), and pores (labeled 'C'). Their three-dimensional shapes can be deduced from these figures. The carbon inclusions of larger size can be described as having a flake-like geometry, whereas the smaller size inclusions have rather irregular shapes and are located at triple junctions and grain boundaries. Similar irregularity was observed in the case of other non-metallic inclusions. It should be noticed that for most of the large carbon inclusions the major axis is oriented almost perpendicular to the hot-pressing direction (Fig. 1b). This will have important implications for the process of failure, as discussed later. The pores, typically smaller than 1 μm and angular in shape, were observed either individually or arranged as clusters. These observations are in line with other boron carbide materials processed by hot-pressing and investigated elsewhere [7,15].

Inclusion morphology and statistics were quantified as follows. A total of 350 images covering an area of ~20 mm^2 was examined. The measurement of the minimum inclusion size in the size distribution was limited by the resolution of the optical microscope, and is ~0.5 μm. The shape factor of the inclusion was determined based on its aspect ratio, $R = a/b$, where a is the longest chord and b is the longest transverse chord (orthogonal to the major chord). Inclusions were also characterized by their surface area, motivated by the irregular shapes of inclusions. The area of the inclusion was determined by a digital image processing system counting all pixels contained in the inclusion. The inclusion contribution (defined by the number and area fraction) to the inclusion size distribution (described by the major chord) was determined by the number/area of this inclusion divided by the total number/area of all inclusions.

Figure 2a shows inclusion number/area fraction versus inclusion size distribution as determined by the image analysis. There is a noticeable difference between these two distributions (number fraction and area fraction), as is to be expected. A large number of small-size inclusions present in the microstructure significantly contribute to the number-based distribution, whereas their measured total surface area is small in the area fraction distribution. The average number-weighted size of inclusion was estimated to be approximately 2 μm, while area-weighted size was about 7 μm. Regardless of the distribution of the inclusions size, the vast majority of identified inclusions were smaller than the average boron carbide grain size (which is ~15 μm). The fraction of large inclusions is small, but important.

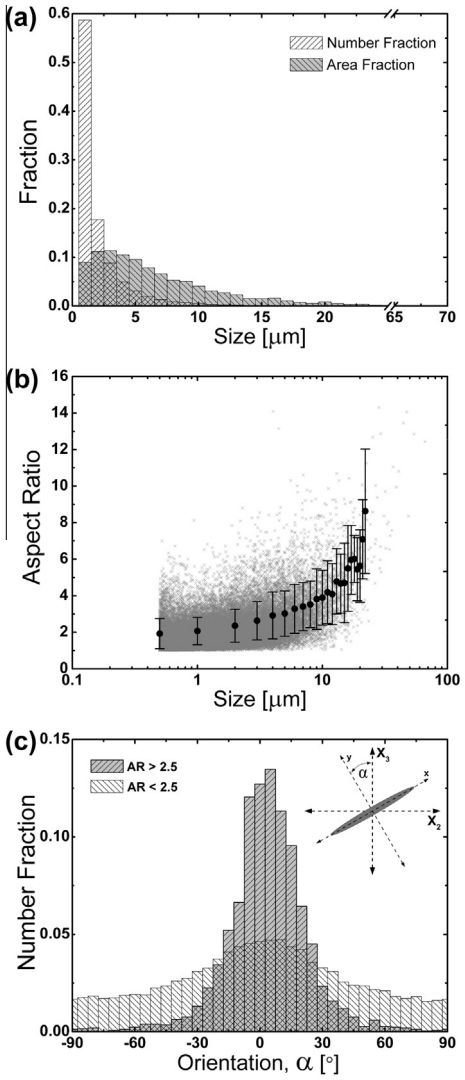

Figure 2. (a) Inclusion number/area fraction versus inclusion size distribution; (b) scatter plot of identified inclusions with a correlation between the aspect ratio and sizes; (c) orientation of inclusions in relation to the major X_3 axis, where AR is the aspect ratio.